Electronic and magnetic properties of electron-doped V_2O_5 and NaV_2O_5

Churna Bhandari and Walter R. L. Lambrecht
Department of Physics, Case Western Reserve University, Cleveland, Ohio 44106-7079, USA
(Received 26 June 2015; published 17 September 2015)

Because of its narrow split-off conduction band, doping of V_2O_5 leads to interesting strongly correlated electrons. We study the effects of doping on V_2O_5's electronic and magnetic properties, either by adding electrons compensated by an artificial homogeneous background, or a virtual crystal approximation (VCA), by changing the atomic number Z_V, so as to keep charge neutrality, or by explicitly introducing Na as a dopant. The former two are considered as a way to simulate injected charge by gating, the latter occurs in the vanadium bronze NaV_2O_5. We also simulate $Na_{1-x}V_2O_5$ using a virtual crystal approximation by changing the atomic number $10 \leqslant Z_{Na} \leqslant 11$. The differences in the band structure, which result from how the electrons added to the band are compensated by positive charge in the three models, are compared. The electronic band structures are calculated using the quasiparticle self-consistent $QSGW$ method including a lattice polarization correction and the local spin density functional method with Hubbard-U corrections (LSDA+U). For NaV_2O_5, the half-filling leads to a splitting of the up- and down-spin lowest d_{xy} band. The spins are found to prefer an antiferromagnetic ordering along the chain direction. Other spin configurations are shown to have higher energy and the exchange interactions are extracted and compared with literature. The optical conductivities are calculated and compared with experiment. Similar results are found for simply doping the band compensated by a background or virtual crystal approximation. However, the position of the occupied bands depends on the method chosen for compensating the charge. The most realistic way to simulate gating in which the compensating charge is kept away from the V_2O_5 layer is the VCA with varying Z_{Na}. The splitting between the up- and down-spin bands depends on the filling. We find that below a certain concentration of about 0.88 electrons per V, the FM arrangement becomes preferable over the antiferromagnetic one. The magnetic moments then gradually decrease as we lower the filling of the split-off band.

DOI: 10.1103/PhysRevB.92.125133 PACS number(s): 71.20.Ps, 73.21.−b

I. INTRODUCTION

A unique feature of V_2O_5, a layered material with weak interlayer van der Waals bonding, is that its lowest conduction band is separated from the rest of the conduction bands by a gap of about 1 eV and has essentially one-dimensional dispersion. The origin and dispersion character of this split-off narrow band is closely related to the unique structure of V_2O_5, which consists of chains within each layer. As explained in detail in our recent paper [1] and elsewhere [2,3], the split-off band corresponds to V-d_{xy} orbitals, with xy in the plane of the layer, which do not have an antibonding interaction with the bridge oxygen linking the two chains. All other V-d orbitals have antibonding interactions with O-2p orbitals and thus lie at higher energy. In pure V_2O_5, this circumstance is of little importance because the band is empty. However, as soon as we add electrons to this band by doping, interesting effects can be expected. That is the reason why in this paper we study doping of V_2O_5.

The doping of V_2O_5 is expected to play a significant role in various of its existing and potential applications. These include catalysis [4,5], Li-ion batteries [6,7], electrochromic devices [8], and electrooptical switching devices [9]. The catalytic properties in oxidation reactions are in part related to the vanadyl oxygens, which are bonded to a single V. Removing this oxygen also dopes the lowest conduction band [10]. However, alkali intercalation also plays a role in certain catalytic activities [5]. Li and other alkaline metals can be intercalated in the structure, and may find interesting ionic conduction channels in V_2O_5 nanostructures but also dope the system with electrons. Nanostructuring of V_2O_5 has been explored recently in designing new types of Li ion batteries. From a fundamental science point of view, alkali and alkaline-earth intercalated V_2O_5, in particular NaV_2O_5 have attracted great attention as so-called ladder compounds [2,11], as discussed in detail below.

In a usual semiconductor, doping is mostly viewed as facilitating the transport by adding mobile electrons or holes in an otherwise empty or filled band. However, even at fairly high doping levels, one usually considers the bands themselves as fixed. In other words, one adopts a rigid band model. This is not entirely correct, but the deviations from rigid band behavior are small. It is well known, for example, that electron-interaction effects reduce the band gap slightly when the band is filled degenerately up to a Fermi level [12–14]. Also, the Moss-Burstein effect [15,16] of band filling on the optical absorption are well known. However, in V_2O_5, the lowest split-off narrow conduction band may be expected to become strongly modified by doping since the doping can fill a sizable fraction of the band. We are then faced with a narrow band with strong on-site Coulomb interactions because of the d character of the band. This situation leads to strong correlations and possibly magnetic effects. In addition, new optical absorption channels between the partially filled V-d lowest band and the higher empty d bands in the infrared and visible are probably involved in the electrochromic activity.

There are several possible routes to doping V_2O_5. The one mostly explored in the past is intercalation with alkali and alkaline earth ions. There have been several studies of V_2O_5 doped with various alkali or alkaline metals and even noble metals such as Li [17], Cs [17,18], Na [19], K [19], Ag [20],

Mg [17], Ca [17], and Ag [21]. These materials are called vanadium bronzes. Some of these dopants perturb the crystal structure significantly from its native layered structure. For example, as one increases the concentration of Li in V_2O_5, several phases form. However, we are here only interested in the cases where the layered structure stays intact, except that the intercalates may somewhat extend the distance between the layer. This is the case of α'-NaV_2O_5. This material is an example of a so-called quarter filled ladder compound as explained in the next paragraph.

In fact, NaV_2O_5 corresponds to doping of 1 electron per two d_{xy} orbitals, so a quarter filling of the corresponding bands. Since only one of those bands is split off from the rest of the conduction band continuum, it means the split-off band is half filled. Furthermore, this band has dispersion essentially only along the chains. This is then a half-filled Hubbard chain, and thus we indeed expect interesting correlation effects and antiferromagnetic ordering. NaV_2O_5 has indeed been reported by Carpy *et al.* [22] to have an antiferromagnetic susceptibility with a an estimated Néel temperature of $T_N \approx 320 \pm 50$ K. Because of the one-dimensional character, the ordering is not perfect and is probably accompanied by significant spin fluctuations even at fairly low temperature.

At 34 K, a phase transition has been found in α'-NaV_2O_5 to an even more interesting state [11]. It was first thought to be a spin-Peierls (SP) transition. The spin-Peierls transition corresponds to the dimerization of an antiferromagnetic 1D Heisenberg ($S = 1/2$) chain. It corresponds to the formation of a minimum energy or gap for the spin-wave excitations. A historical review on the subject can be found in Jacobs *et al.* [23] Theoretically, it arises in the context of finding the ground state and low energy excitations of one-dimensional spin systems. Important papers on this subject include Bonner and Fisher [24], Bulaevski [25], Haldane [26,27]. Experimentally, such transitions were first observed in organic systems [23], and subsequently in $CuGeO_3$ [28]. It was then reported to occur in α'-NaV_2O_5 by Isobe and Ueda [11]. However, the spin Peierls model in α'-NaV_2O_5 was based on the assumption of a separate V^{4+} ($S = 1/2$) and V^{5+} ($S = 0$) chain corresponding to a noncentrosymmetric orthorhombic crystal structure with two inequivalent V and 5 inequivalent O sites, as determined by Carpy *et al.* [22]. The latter was found to be incorrect by more accurate structure determinations [2,29]. The structure, at least above the transition temperature, was found to be centrosymmetric P_{mmn}, which is the same space group as pure V_2O_5 and a single spin was argued to occupy each V-O-V "rung" in a quarter filled ladder compound is a sort of molecular state.

Because of this finding, the phase transition was then argued to consist of a charge ordering (CO) [30], or possibly a charge ordering followed immediately by a spin-Peierls transition [31]. In fact, the centrosymmetric P_{mmn} structure was found to be no longer stable at low temperature. For instance, nuclear magnetic resonance (NMR) measurements show that there are two inequivalent vanadium sites below $T = 34$ K one electron being localized in the $3d_{xy}$ state of one vanadium ($S = 1/2$) and another being empty non-magnetic ($S = 0$) in a rung, which clearly implies that the NaV_2O_5 undergoes to a charge ordering phase transition. In fact, similar charge ordering is also revealed by x-ray diffraction [32] and dielectric [33] studies. Although a low-temperature structure was determined by Ludecke *et al.* [32], there is still a controversy about the charge ordering whether it occurs in every vanadium ladder [30] or in every other ladder [34,35]. There also is still some controversy about the nature of the ground state of the electrons in the V-O-V rungs, for which different results are obtained within open-shell Hartree-Fock and configuration interaction based cluster models [34,36]. Such models assign an important contribution to the singly occupied O^{bridge} p_y orbital configurations, while DFT-based models consider this orbital always doubly occupied.

In the present paper, however, we will not delve into the nature of the low-temperature phase but focus on the antiferromagnetic state above 34 K. Instead, our focus is on different approaches to doping and their effect on the electronic band structure.

Experimentally, other approaches to doping or "reduction" of V_2O_5 to a lower oxide exist. It is pretty easy to see that vanadyl oxygen vacancies would dope the split-off band. Vanadyl oxygens are the oxygens that are bonded to one V via a triple bond. Breaking the bonds of this oxygen to V would mainly lower the $d_{3z^2-r^2}$ and d_{xz}, d_{yz} orbitals but these lie well above the d_{xy} derived split-off band so its electrons will dope the split-off band without introducing levels below it. This type of doping leads to lower oxides if the vacancies order and has also been studied to some extent although their electronic structure has not been fully explored. Studies of oxygen vacancies in V_2O_5 can be found in Scanlon *et al.* [37] and Xiao *et al.* [10].

With the recent developments in fabricating ultrathin films of only a few atomic layers thick, for example, by exfoliation, as used in graphene and transition-metal dichalcogenides, another way of controlled doping becomes possibly available. These are thin enough that gating by means of a control electrode on the back side of the substrate on which the thin-film material is placed allows one to inject a sizable fraction of electrons in the material. Other possibilities for applying a higher field to the layer include electrolytic double layers on the surface or possibly a scanning tunneling microscope tip. A doping of one electron per V_2O_5 formula unit corresponds to 5×10^{14} e/cm^2. This is large but possibly within reach for a thin enough layer. The main advantage of this approach would be that doping could be pursued continuously without at the same time introducing scattering centers and disorder in the film itself. It is similar in that sense to the approach of delta doping in semiconductor heterojunctions. It could also be used in conjunction with intercalation. For example, one might envision placing an atomically thin mono- or few-layer V_2O_5 sample on an alkali metal covered surface and then with a bias voltage reducing or enhancing the carrier concentration in the layer.

Our focus in this paper is to compare this situation with doping by means of intercalation. In order to simulate additional electrons in the layer, we need to maintain charge neutrality. We can do this in two ways, either by adding a corresponding compensating homogeneous background, or by a so-called virtual crystal approximation (VCA), in which we replace the V core charge by a fractional number. For example, to add 0.1 e per V, we would add 0.1 to the atomic number of V. The approach with homogeneous background means that

the corresponding positive charge is in part situated in the interstitial region between the layers, but also in part in the layer itself. On the other hand, in the case of actual doping by alkali metals such as Na, the positive Na^+ ions are also situated in the interstitial region but in a discretized rather than continuous manner. The Na indeed creates energy levels high in the conduction band and just donates electrons to the system. We found that the split-off bands have negligible contribution from Na. However, Na also modifies the structure slightly. Mostly, it increases the c lattice constant, or distance between the layers. We have previously studied how increasing the c spacing between the layer affects the electronic structure in our study of monolayer V_2O_5. Thus our goals are to compare the different ways in which these different approaches to doping affect the band structure.

In particular, we focus on the energy region of the split-off bands and the gap. To the first approximation, what one expects is that for half-filling of this band, it may become favorable to split the band into its spin-up and -down parts and in other words create a magnetic moment if the Stoner criterion is satisfied. However, the question then becomes: does the material become ferromagnetic or antiferromagnetic and what is the preferred way of ordering the moments? This situation corresponds closely to that of NaV_2O_5 in the antiferromagnetic phase. We thus examine it first and make contact with the previous studies of this material. Next, we investigate to what extent a similar band splitting and magnetism occur for doping without Na but using the background approach or VCA. Finally, since the latter allows to add arbitrary density of additional electrons, we can study whether the magnetic phases persists for lower electron doping concentrations. This could in principle also be done by using $Na_xV_2O_5$ and in fact concentrations $0.9 < x < 1$ have been explored experimentally. However, here we also want to consider even lower concentrations. We can again do this within a VCA by using $Z = 11 - x$ for Na.

Although several previous studies of NaV_2O_5 made use of the LSDA+U approach, i.e., local spin density approximation with Hubbard-U corrections, the quasiparticle self-consistent $QSGW$ approach, which we applied recently [1] to V_2O_5, has not yet been applied to this material and may offer new insights because it provides a parameter free and starting point independent approach to the quasiparticle excitations. Nonetheless, in order to obtain a suitable starting point which already includes the expected spin splittings, we will use LSDA+U. We emphasize that the final result however, is independent of this starting point.

As in our previous work [38], we find that $QSGW$ significantly overestimates the band gap for V_2O_5, which is attributed in most part due to the missing lattice polarization effect in the screened Coulomb interaction W. We therefore estimate the lattice polarization effect using published results on the LO-TO splittings in NaV_2O_5. Essentially, this leads to a strong reduction in the GW self-energy. As a result, LSDA is actually remarkably accurate for V_2O_5. Still, we will show it is important to go beyond it to include the correlation effects in the split-off d bands. These are, in effect, the main focus of the paper.

The paper is organized as follows. In Sec. II, we revisit the first principles approximations such as LSDA+U and $QSGW$. The Sec. III is split in several sections. First, in Sec. III A we review the structure and our structural relaxation results. Next, in Sec. III B, we focus on NaV_2O_5. In this section, we first discuss band structure at different computational levels, then the optical properties and finally the magnetic exchange interactions. In the next Sec. III C, we discuss alternative models for doping, such as the homogeneous background and virtual crystal approximation, and finally, we apply these methods to varying doping levels. In Sec. IV, we conclude this work.

II. METHODOLOGY

The full potential linear muffin-tin orbital (FP-LMTO) [39,40] method is used to solve the density functional Kohn-Sham eigenvalue problem within the local density approximation (LDA) [41,42], or the local spin density approximation (LSDA) with Hubbard U corrections (LSDA+U) as well as the quasiparticle equation in the $QSGW$ approximation. The implementations used are available in Refs. [43,44]. In the FP-LMTO method used [39], the basis set is specified by two sets of parameters, the smoothing radii R_{sm} and decay lengths (κ) of smoothed Hankel function envelope functions. For NaV_2O_5, we include (spd, spd) for V, (spd, sp) for O, and (sp, s) for Na atoms, respectively. These indicate the angular momenta included for each κ. The envelope functions are augmented inside the spheres in terms of solutions of the Schrödinger equation and their energy derivative up to an augmentation cutoff of $l_{\max} = 4$.

The Brillouin zone integration **k**-point convergence and other convergence parameters of the method were carefully tested in our previous work of V_2O_5 and similar criteria were adopted here. Specifically, we use a $2\times6\times6$ unshifted mesh for the Brillouin zone of the standard unit cell, along with the tetrahedron method for the metallic cases in the LDA self-consistent charge convergence. A slightly coarser sampling $1\times3\times3$ was adopted for the calculation of the Σ in GW but the latter is interpolated to the finer mesh or the **k** points along symmetry lines in plotting the GW bands. For the antiferromagnetic cell doubled in the b direction, we use a correspondingly smaller number of **k** points, $2\times4\times6$ in LDA and $1\times2\times3$ for $QSGW$.

As already mentioned in the introduction, one expects that the half-filled narrow band may become spin-split. Therefore we need to include spin polarization. In some cases, however, the LSDA functional is not sufficient to create the splitting. Therefore we use the LSDA+U method, which adds an orbital dependent stronger Coulomb interaction U to the d states. The smallest possible U providing a splitting was used. In fact, for the antiferromagnetic case, or in case of background doping, a splitting of the bands already occurred within LSDA without need for adding U. We stress, however, that we use this only as a starting point for the $QSGW$ calculations. The results or the latter are independent of the starting point and the GW self-energy in the end replaces the additional potentials from the LSDA+U in going beyond LSDA. The quasiparticle self-consistent $QSGW$ method is described in detail elsewhere [45–47]. The implementation parameters used here are similar as in our previous study of the band structure of bulk and monolayer V_2O_5 [1].

As mentioned earlier, in order to simulate doping by gating, we wish to add electrons without adding specific dopants. To keep the system neutral, we employ two different approaches, either add a homogeneous background (QB) or we distribute the counter charge over the nuclei of the V_2O_5. Although, this is not the only possible choice, we only modify the atomic number Z_V of the vanadium atoms.

III. RESULTS

A. Structure of NaV_2O_5

As already mentioned, there have been numerous studies of NaV_2O_5 in particular to elucidate the low temperature phase. The first experimentally proposed structure [22] at room temperature has the noncentrosymmetric P_{2_1mn} space group with two vanadium and 5 oxygen inequivalent sites. However, this structure was refuted by later experimental results. Instead a centrosymmetric structure [2] was found at room temperature. This crystal structure is orthorhombic with the P_{mmn} space group with one vanadium and three inequivalent oxygen sites as in pure V_2O_5 crystal. The unit cell is shown in Fig. 1 and contains two formula units or a total of 16 atoms: 2 Na, 4 V, and 10 O atoms. The lattice constants are slightly changed from pure V_2O_5, for example $a = 11.315$ Å [2] (11.512 Å) [48], $b = 3.61$ Å (3.56 Å), and $c = 4.80$ Å (4.37Å), where the numbers in parenthesis refer to pure V_2O_5. This amounts to -1.7%, 1.4%, and 9.8% changes in a, b, and c, respectively. Clearly the c lattice constant increases the most. This also leads to a rotation of pyramids surrounding each V because the apical (vanadyl) oxygen anions are attracted towards the Na cation. This implies that some more intermixing of the different d-orbital types will occur.

We first carried out structural optimization in LDA for the NaV_2O_5 case. To avoid the typical underestimate of experimental lattice constants in LDA, and the difficulties of standard density functionals to optimize the distance between Van der Waals bonded layers, we adopt the experimental lattice constants. Only the atomic internal coordinates were relaxed. The relaxation is carried out until the forces are less than 10^{-3} Ryd/Bohr. As shown in Table I, the bond lengths of various atoms in NaV_2O_5 slightly underestimate the experimental values. The bond lengths of Na to V or O correspond to nearest-neighbor distances. Corresponding results for pure V_2O_5 were reported in Ref. [1].

TABLE I. Bond lengths in angstroms.

	V-O_v	V-O_{cy}	V-O_{cx}	V-O_b	Na-O_b	Na-V
Our	1.62	1.89	1.99	1.80	2.42	3.32
Expt.[a]	1.61	1.92	1.99	1.82	2.43	3.35

[a]By Smolinski *et al.* [2].

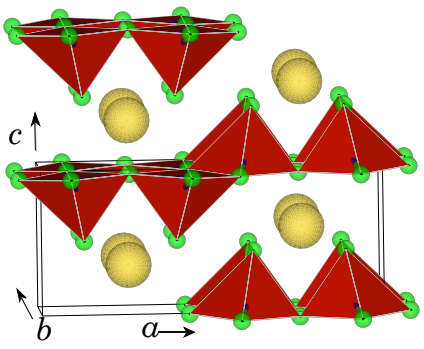

FIG. 1. (Color online) Crystal structure of NaV_2O_5 showing edge shared polyhedra alternatively pointing up and down. Here the blue spheres represent V, the yellow Na, and the green O atoms respectively.

B. Band structure of quarter-filled NaV_2O_5

We start our study with NaV_2O_5. First, we carried out non-spin-polarized (LDA) as well as spin-polarized (LSDA) and LSDA+U calculations for hypothetical ferromagnetic (FM) and the actual antiferromagnetic (AFM) structure, which has alternating spin-up and spin-down along the chains in the b direction and parallel spins for V atoms in a bridge and for the two double chains occurring in the standard V_2O_5 unit cell. Additional antiferromagnetic arrangements were also considered.

1. Non-spin-polarized band structure

The non-spin-polarized band structure and density of states is shown in Fig. 2. As anticipated, the band structure looks very similar to that of pure V_2O_5 with the difference that now the Fermi level is placed inside the split-off conduction band and is in fact precisely half-filled. The density of V-d like states at the Fermi level $D_{V-d}(\epsilon_F) = 0.657$ states/eV/spin and does not satisfy the Stoner criterion $ID(\epsilon_F) > 1$ with the Stoner $I = 0.354$ eV for vanadium taken from Janak [49]. Correspondingly, we indeed find that within LSDA, no magnetic moment forms and the band structure stays non-spin-polarized. However, within LSDA+U with a $U_{\text{eff}} = U - J \approx 2.7$ eV, splitting of up- and down-spin states occurs and subsequently we can apply $QSGW$ and find that the formation of a magnetic moment persists. The value of U_{eff} is not critical. The value chosen here is chosen to mimic the results of the final $QSGW$ as best as possible for the AFM case.

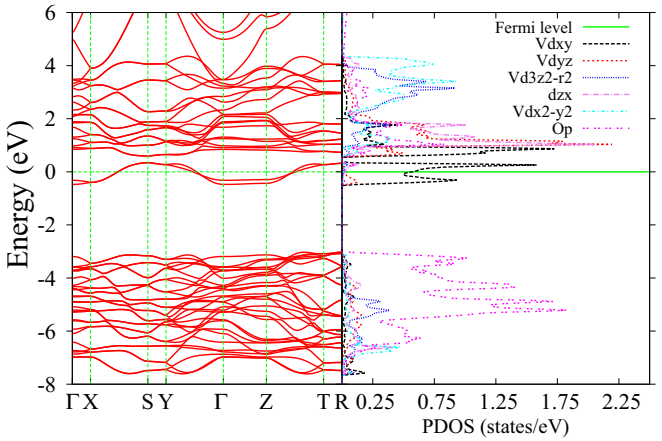

FIG. 2. (Color online) Non-spin-polarized LDA calculation of NaV_2O_5 bands and density of states.

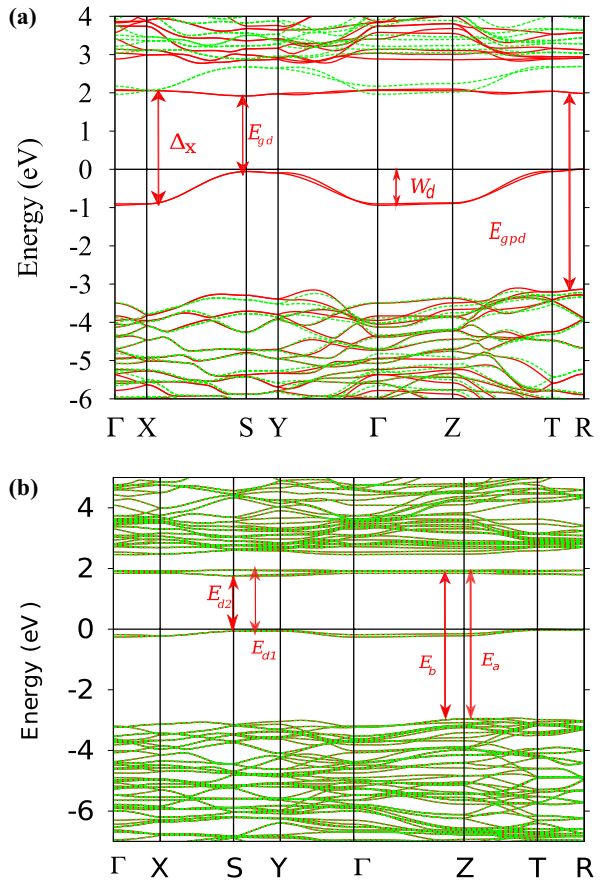

FIG. 3. (Color online) Band structures of NaV_2O_5 obtained in the $QSGW$ approach for (a) ferromagnetic and (b) antiferromagnetic ordering of the moments. Red solid lines indicate majority spin and green dashed line minority spin bands.

The antiferromagnetic structure could in fact be stabilized even in LSDA without any U. As will be shown below, the antiferromagnetic ordering of these moments along the b axis is preferred. However, before delving into the magnetic total energy differences, let us first discuss the band structure.

2. QSGW band structures in AFM and FM cases

The $QSGW$ bands of FM and AFM NaV_2O_5 are shown in Fig. 3. As for pure V_2O_5, we first notice a strong increase in the gap between O-2p valence bands and the bottom of the conduction bands (not counting the spit-off band) to an unrealistic value of about 5 eV. This is even larger than in pure V_2O_5, which results from the larger interlayer distance or the increase in the c lattice constant by almost 10%. We also see that the split-off band splits in up and down spin and the filled majority spin band is pushed down to about 2 eV below the continuum of d-conduction bands. One may recognize a corresponding minority spin band with almost identical dispersions. We call the more or less constant splitting between these two bands Δ_x, the exchange splitting of the band. It is indicated in Fig. 3 along with other splitting discussed later. Obviously, in the LSDA+U approach, its value increases with the choice of U but it is not exactly equal to U. However, we also see a majority spin very flat band at 2 eV, which is the second d_{xy} like band, which has antibonding interactions with the bridge oxygen but which is shifted down by the exchange interaction with the spin polarization of the other d_{xy} band. In other words, the spin polarization of the split-off band results in an induced spin splitting in all the higher lying d bands. We can indeed see a splitting of up and down spin bands throughout the conduction band. In other words, we produced a ferromagnetic insulator instead of a metallic band structure. However, as will be discussed later, this is not the lowest-energy structure because the spins prefer an AFM ordering along the chain.

Now, if we go to the AFM case, a similar gap structure occurs. There is a gap of about 3 eV between O-2p VBM and the lowest filled d states. Then there is a gap of about 2 eV to the next empty states. A new set of four empty bands is split-off by about 0.4 eV from the continuum of d bands. This is again the same splitting as we saw before for the FM bands and results from the induced spin-polarization in the higher d bands. Remarkably, however, the dispersion of the filled split-off band is now strongly reduced. The bandwidth of the FM split-off band was about 1 eV but in the AFM case it is reduced to only about 0.2 eV. This results from the fact that in a collinear spin calculation, hopping only occurs between orbitals of the same spin and so along the chain direction, the nearest neighbor V hopping is now suppressed and only much weaker second nearest-neighbor hopping contributes to the band width. If we examine this band structure as function of $U_{\rm eff}$ in LSDA+U, we find that the splitting between the first empty and first occupied d band stays more or less constant but the splitting between the filled d band and the empty d band continuum increases, so the filled band gets pushed closer to the O-2p bands. This is because the larger U, the more the occupied spin states are pushed down but the lowest separate set of empty bands are not the corresponding opposite spin bands but rather the d_{xy} bands that are antibonding with bridge O-p_y.

3. QSGW with lattice polarization correction

The $QSGW$ band structure in this material is quite unrealistic and as we proposed in Bhandari *et al.* [1] for pure V_2O_5, which can be largely attributed to the importance of lattice polarization contributions to the screening of W in these materials. This results from the strong LO-TO splitting of the phonons. The LO phonons lead a contribution to the dielectric screening for long wavelengths ($\mathbf{q} \to 0$ limit), which affects the screening of the electron-electron interaction even though the LO phonons are much lower frequency than the electronic inter-band transitions. The generalized Lyddane-Sachs-Teller relation gives this increase in the screening due to lattice polarization as

$$\varepsilon^{\alpha}_{\rm tot}(\mathbf{q}\to 0,\omega) = \varepsilon^{\alpha}_{el}(\mathbf{q}\to 0,\omega)\prod_i \frac{\omega^2_{\rm LOi}-\omega^2}{\omega^2_{\rm TOi}-(\omega+i0^+)^2}, \quad (1)$$

where the product is over all modes corresponding to the irreducible representation to which the Cartesian component α belongs. In practice, we estimate this effect by taking the $\omega \to 0$ limit and assuming that the GW self-energy shift $\Delta\Sigma$ is dominated by the static screened exchange contribution. Thus we multiply $\Delta\Sigma$ by a reduction factor $\alpha = \varepsilon_{el}/\varepsilon_{\rm tot}$ To take in to account the anisotropy, we average over directions by multiplying the Cartesian components and taking the cube

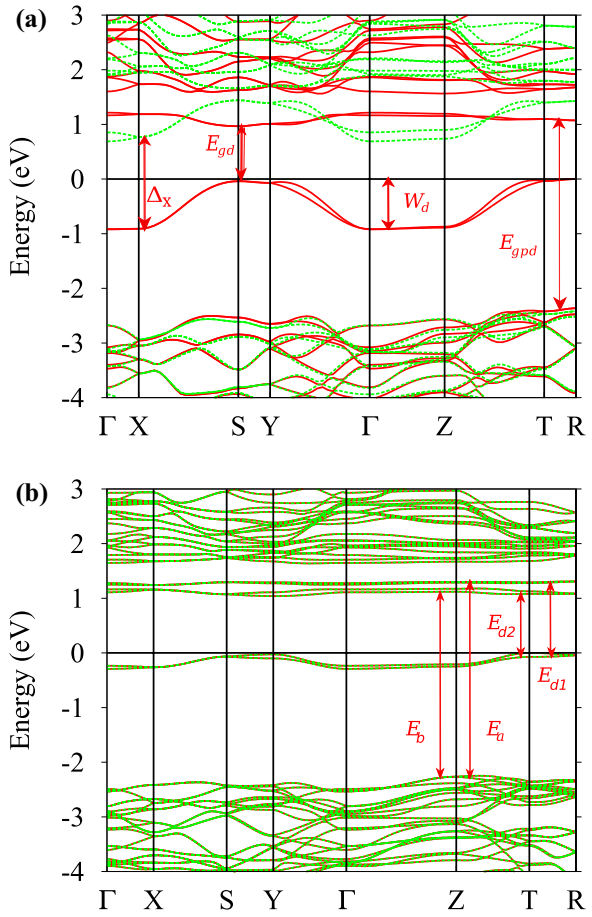

FIG. 4. (Color online) Band structures of NaV_2O_5 obtained in the $QSGW$-$\alpha\Delta\Sigma$ approach with $\alpha = 0.38$ for (a) ferromagnetic and (b) antiferromagnetic ordering of the moments.

root. In pure V_2O_5, this led to a reduction factor of $\alpha = 0.38$. In the present case, using phonons for NaV_2O_5 as reported in Popova *et al.* [50], we obtain a reduction factor $\alpha = 0.5$. The phonons in V_2O_5 and NaV_2O_5 are indeed very similar and this difference should be considered to be within the uncertainty of the approach, which is only a crude way of estimating the lattice polarization effect to begin with. We thus keep the $\alpha = 0.38$ as in our previous V_2O_5 calculation for easier comparison.

The corresponding band structures are shown in Fig. 4. The gap between the O-2p like VBM of V_2O_5 and the lowest now filled V-3d band is about 1.81 eV and the gap between the filled d band (new VBM) and the empty d bands is now about 1–1.3 eV, slightly lower in the FM than in the AFM case. Also note that in the FM case, the lowest gap is indirect between the majority spin filled split-off band at S and the corresponding minority spin band at Γ. However, the lowest direct allowed transitions would be between the majority spin bands at S. The splitting between up and down spin d_{xy} bands is about 2 eV and is uniform throughout the Brillouin zone. This corresponds to the exchange splitting Δ_x of these bands and justifies the previous use of a $U_{\text{eff}} \approx 2.7$ eV in LSDA+U. In the AFM case, this splitting cannot be so easily identified and the gap between lowest filled and lowest empty d band is slightly larger, about 1.3 eV.

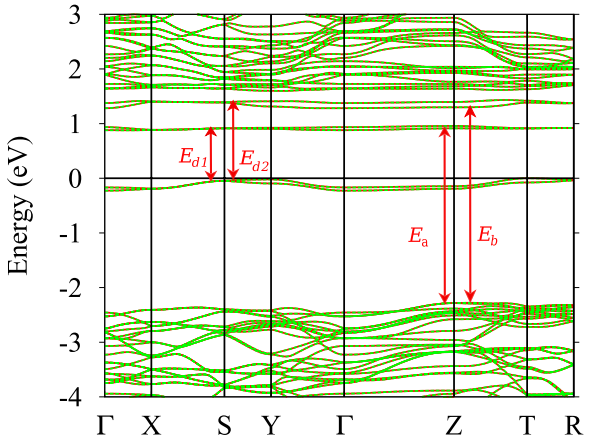

FIG. 5. (Color online) Band structure of AFM NaV_2O_5 within LSDA+U with $U_{\text{eff}} = 2.7$ eV.

There are further small differences between LSDA+U and these 0.38 $\Delta\Sigma$ QSGW results. Overall, similar band structures to ours were obtained by Ming *et al.* using LSDA+U [51]. We include in Fig. 5 our band structure within LSDA+U with $U_{\text{eff}} = 2.7$ eV because it agrees best with optical response as will be shown in the next section. In particular, we may note a slightly larger splitting of the two sets of empty split-off d bands below the continuum of the conduction band.

4. Optical response

We now compare these results with experimental data of the optical conductivity by Konstantinovič *et al.* [52]. Similar results were obtained by Atzkern *et al.* [53] from electron energy loss spectroscopy (EELS) and by Presura *et al.* by spectroscopic ellipsometry [54]. To this end, we calculate the optical conductivity for $\mathbf{E} \parallel \mathbf{a}$ and $\mathbf{E} \parallel \mathbf{b}$, as shown in Fig. 6. We compare both the LSDA+U with $U = 2.72$ eV and the 0.38$\Delta\Sigma$ QSGW with experiments.

Experimentally, a peak in optical conductivity is found at about 1 eV for $\mathbf{E} \parallel \mathbf{a}$ and assigned to transitions between the highest filled and lowest empty V-d states [52]. This agrees well with our calculation, which shows a strong peak at about 1 eV in LSDA+U case but in the 0.38$\Delta\Sigma$-$QSGW$ case, this peak is found a little higher at 1.5 eV. Further inspection of the PDOS (in LSDA+U) shown in Fig. 7 shows that this corresponds to a transition to the V-d_{xy} derived, which forms antibonding interactions with O_{bridge}-p_y. In previous work, this is sometimes called the antibonding xy band.

In a simple tight-binding model, the "molecular" states of the rung, from which the split-off bands are constructed can be described by a Hamiltonian of the form

$$H = \begin{pmatrix} E_d & & V_{dp\pi} \\ & E_d & V_{dp\pi} \\ V_{dp\pi} & V_{dp\pi} & E_p \end{pmatrix}. \quad (2)$$

The basis functions here correspond to d^1_{xy} on the left V atom, d^2_{xy} on the right V atom, and p_y on the bridge oxygen between them. There is only a $V_{dp\pi}$ interaction between the O and V orbitals. One may now downfold the p states into the d-states

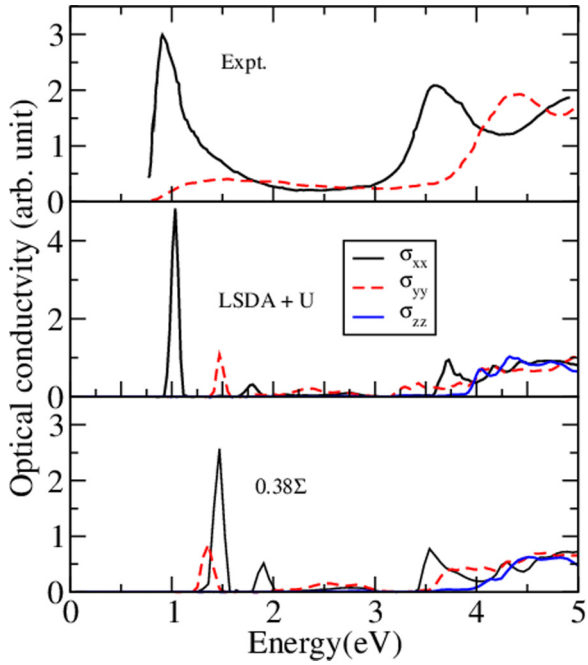

FIG. 6. (Color online) Optical conductivity of AFM1 NaV_2O_5: (top) experiment [53]; (middle) LSDA+U; and (bottom) $0.38\Delta\Sigma$.

to obtain an effective 2×2 Hamiltonian:

$$H_{VV} = \begin{pmatrix} E_d + \frac{V_{dp\pi}^2}{E_d - E_p} & \frac{V_{dp\pi}^2}{E_d - E_p} \\ \frac{V_{dp\pi}^2}{E_d - E_p} & E_d + \frac{V_{dp\pi}^2}{E_d - E_p} \end{pmatrix}, \tag{3}$$

whose eigenvalues finally are

$$E_b = E_d,$$
$$E_a = E_d + 2\frac{V_{dp\pi}^2}{E_d - E_p}. \tag{4}$$

In other words, for the symmetric or bonding combination of the two effective d orbitals, the antibonding interaction with O-p is canceled out. In fact, by symmetry, one can see

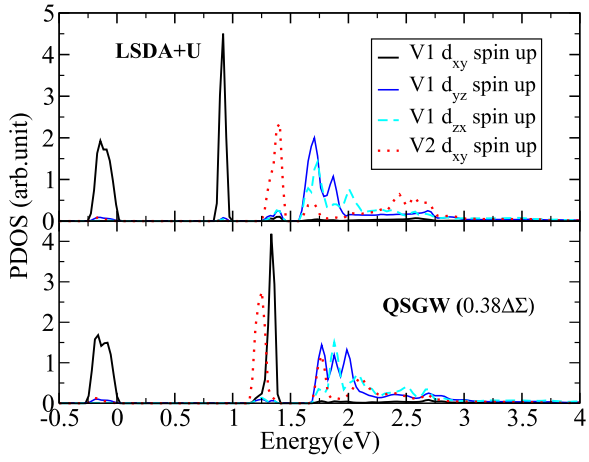

FIG. 7. (Color online) PDOS on V atoms in the filled and empty split-off bands and low conduction bands relevant to the optical transitions obtained top panel in LSDA+U with $U = 2.72$ eV and bottom panel in QSGW $0.38\Delta\Sigma$.

easily that if the two xy orbitals have the same sign, they are antisymmetric with respect to the mirror plane passing through the bridge and therefore do not interact with the O-p_y. The antisymmetric or antibonding combination, however, has twice the antibonding interaction with O-p_y. From this, it becomes clear that for polarization **E** ∥ **a**, which is also antisymmetric with respect to this mirror plane, optical transitions are allowed between these bonding and antibonding xy orbital combinations on the same rung. Apparently, our $0.38\Delta\Sigma$ model slightly overestimates this bonding to antibonding gap, just as it still slightly overestimates the O-2p–V-d gap. This may be because we do not yet fully accurately include the anisotropies of the lattice polarization effect, and/or because of missing electron-hole interaction effects on the screened Coulomb interaction W. The assignment of this peak for **E** ∥ **a** agrees with that by Atzkern *et al.* [53].

This transition is not allowed for **E** ∥ **b** for the symmetry reasons explained above, but we find a weaker transition, which in LSDA+U occurs at slightly higher energy and in $0.38\Delta\Sigma$ occurs slightly below it. Further inspection shows that in LSDA+U, the first narrow set of empty d-bands again split in two, while in $0.38\Delta\Sigma$, they are closer together. Inspecting the PDOS shows that the band corresponding to this transition has opposite spin character to the occupied d band, which is the initial state of the transition. In fact, Atzkern *et al.* [53] assigned this transition to a $d_{xy} \uparrow$ to $d_{xy} \downarrow$ transition. However, without circularly polarized light, there should not be transitions between up and down spin. However, because of the antiferromagnetic order along the **b** axis, or the chain, it means that the atoms along the chain have alternating spin. So, this is in fact a transition from one V to the next V along the chain between states with the same spin. It is now clear why this transition becomes allowed for **E** ∥ **b**.

This transition is indeed seen as a much weaker peak in Fig. 3 of Ref. [52] for **E** ∥ **b** or also in Atzkern *et al.* [53] reproduced here as the upper panel in Fig. 6. The fact that this is an optical transition involving charge transfer from one rung to the next in the ladder explains why it is weaker in oscillator strength than the **E** ∥ **a** transition, which is between molecular states localized on the same rung.

Since this transition is essentially resulting from the spin-splitting of the d band, it is sensitive to the U value chosen, as was found by Atzkern *et al.* [53]. We find this transition at about the same energy in LSDA+U with $U_{\text{eff}} = 2.72$ and in $0.38\Delta\Sigma$, which again justifies the choice of U_{eff} value. The **E** ∥ **a** transition on the other hand was found to be rather independent of U because it results from the bonding to antibonding splitting of the xy bands instead.

At higher energy near 3.5 eV for **E** ∥ **a** and 4.0 eV for **E** ∥ **b** we observe the transitions from the O-2p valence band maximum to these same two bands. We labeled these E_a and E_b and they are listed in the Table II. These peaks are broader and probably also include transitions to the higher-lying d_{xz} and d_{yz} orbitals near the bottom of conduction band continuum. In between the two lowest peaks and the 3.5 eV and beyond ones, we see some small peaks in our calculations, which correspond to the onset of transitions from the occupied d_{xy} band to the continuum of d bands, which is dominated by d_{xz} and d_{yz} like states. A background of transitions is also visible in the experiments. The experimental first peak shows a

TABLE II. Band gaps and other energy differences in NaV_2O_5. Δ_x is the spin splitting of the FM split-off band, E_{gd} is the lowest direct gap between occupied d and empty d states, E_{gpd} is the lowest direct gap between O-2p like VBM and empty d states. W_d is the width of the split-off majority spin band, E_{d1} is the gap between occupied d_{xy} and empty antibonding d_{xy} bands; E_{d2} is the gap between occupied $d_{xy}\uparrow$ and $d_{xy}\downarrow$ on the same atom, E_a and E_b are the transitions from the O-2p VBM to the same final states. The calculated transitions are indicated in the band figures. The corresponding experimental features E_{d1}, E_a and E_{d2}, E_b correspond to peaks for $\mathbf{E} \parallel \mathbf{a}$ and $\mathbf{E} \parallel \mathbf{b}$, respectively. All energies are in eV.

	FM				AFM			
Method	Δ_x	E_{gd}	E_{gpd}	W_d	E_{d1}	E_{d2}	E_a	E_b
$QSGW$	2.96	1.97	5.21	0.91	1.90	1.81	4.97	4.83
$0.38\Delta\Sigma$	1.68	1	3.5	0.91	1.36	1.14	3.72	3.50
$0.5\Delta\Sigma$	1.93	1.25	3.76	0.92	1.40	1.22	3.89	3.69
LSDA+U[a]	1.66	0.48	3.10	0.86	0.92	1.32	3.26	3.74
LSDA					0.48	0.84	3.25	3.62
Expt.[b]					0.9	1.2	3.25	3.9

[a] $U = 2.72$ eV.
[b] From Ref. [52].

marked asymmetric broadening. Atzkern *et al.* [53] attempted to explain this in terms of spin-wave fluctuations away from the perfect antiferromagnetic ordering. They considered spiral spin waves which indeed broaden the majority spin occupied split-off d band. However, they were still not able to fully account for the line shape of this peak.

In Kontantinovič *et al.*'s work [52], additional features are seen in the optical conductivity, which were interpreted as transitions to an impurity band in between the lowest empty d and filled d bands. This impurity band occurs only when the Na concentration is less than 100 %. However, the second empty split-off band in the antiferromagnetic case, which we here interpreted as the opposite spin counterpart to the bonding xy band, was not identified before. Finally, we summarize the band gaps and splittings in NaV_2O_5 obtained in different approximations in Table II for both the FM and AFM case. Even though the FM is not found to occur experimentally, it is important because potentially it could be realized by placing the sample in a saturating magnetic field and may occur for significantly lower Na concentrations as we will discuss below.

TABLE III. Total energies of different magnetic configurations relative to the ground state. The V atoms in the 1×2×1 cell are labeled in Fig. 8.

	1	2	3	4	1'	2'	3'	4'	ΔE (meV)
NM									160
FM	↑	↑	↑	↑	↑	↑	↑	↑	139
AFM1	↑	↑	↑	↑	↓	↓	↓	↓	0
AFM2	↑	↓	↑	↓	↓	↑	↓	↑	717
AFM3	↑	↓	↓	↑	↑	↓	↓	↑	713
AFM4	↑	↑	↓	↓	↓	↓	↑	↑	4

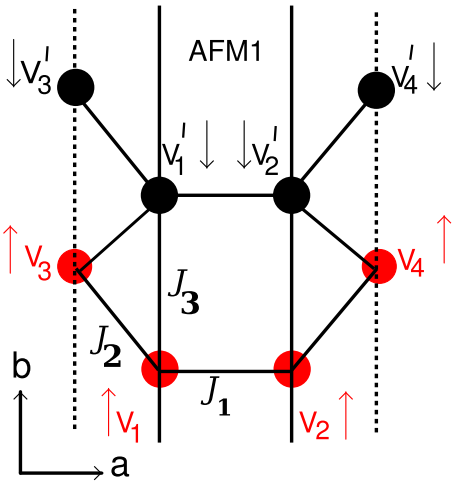

FIG. 8. (Color online) AFM1 spin configuration and labeling of the V atoms. V_1-V_2 form the central rung connected by a bridge oxygen. In the AFM1 model, the V_{1-4} atoms (red) have opposite spin of the V'_{1-4} atoms. The exchange interactions are indicated.

5. *Antiferromagnetic ordering and exchange couplings*

Now, we address the total energy differences between different magnetic configurations and the exchange interactions. These were calculated within the LSDA+U approach with $U_{\text{eff}} = 2.72$ eV. First, in Fig. 8, we show the experimentally occurring AFM structure, which we label as AFM1. We number the V atoms 1-4 and 1′-4′ as indicated to identify the other spin configurations considered in Table III.

These energy differences can be described by a generalized Heisenberg Hamiltonian of the form

$$H = -\sum_{i \neq j} J_{ij} \mathbf{e}_i \cdot \mathbf{e}_j, \tag{5}$$

where the sum is over both i and j, so it counts each neighbor pair twice and the spins are represented as classical unit vectors. This means the magnetic moments are folded into the definition of the J_{ij}. The magnetic moments here are found to be about 0.5 μ_B/V for AFM, which indicates single electron occupation per rung or V pair. The net moments are found to be slightly larger in the FM than in the AFM case. We include the exchange interactions J_1 with $n = 1,2,3$ as follows: J_1 is between V_1 and V_2, J_2 between V_1 and V_3, and J_3 between V_1 and V'_1. The total energies of the eight-vanadium-atom cell of each of the configurations are then given by

$$\begin{aligned} E(\text{FM}) &= -8J_1 - 16J_2 - 16J_3, \\ E(\text{AFM1}) &= -8J_1 + 16J_3, \\ E(\text{AFM2}) &= 8J_1 + 16J_3, \\ E(\text{AFM3}) &= 8J_1 + 16J_2 - 16J_3, \\ E(\text{AFM4}) &= -8J_1 + 16J_3. \end{aligned} \tag{6}$$

We see that within the model up to third neighbor interactions AFM4 and AFM1 have the same energy. In our calculations, they differ by only 4 meV. Even if one would include a J_4 between V_1 and V_4, they would still be equal. So they differ only by some further range interaction. Within this model,

we can extract three energy differences and hence the three exchange parameters.

We see immediately that $E(\mathrm{AFM2}) - E(\mathrm{AFM1}) = 16J_1$ and hence J_1 is 44.8 meV. This indicates a strong ferromagnetic coupling between the two V in the same rung. This is not surprising. In fact, if one thinks of the half-filled ladder as only having one electron in each rung spread over the two V atoms, then obviously, they must have the same spin. On the other hand, we readily find $J_2 = -4.5$ meV and $J_3 = -2.1$ meV. Thus both of these interactions are antiferromagnetic and the they fall off as function of distance. It indicates that the neighboring chains want to be antiferromagnetically coupled as well as the ordering inside the chain tends to be antiferromagnetic. The last conclusion agrees with the study by Atzkern *et al.* [53]. These authors started from the AFM1 observed structure and within LSDA+U extracted exchange interactions from the spin-wave excitations.

The antiferromagnetic interaction J_3 between atoms along the chain can be thought of as superexchange via the chain oxygens connecting the V atoms. More precisely they interact via the $pd\pi$ interaction with $\mathrm{O}^{\mathrm{chain}}$-$p_x$. We obtain a superexchange interaction here, because the bonding xy band of each spin is exactly filled. On the other hand, the exchange interaction J_2 between adjacent ladders cannot be mediated by indirect superexchange because V_3-$\mathrm{O}^{\mathrm{chain}}$-$\mathrm{V}_1$ form close to a right angle, and thus the electron could for example hop from V_1 to a O-p_y but then this y orbital is orthogonal to the xy on the V_3. However, these two V are close enough to have a direct exchange interaction. If they have sufficient overlap then the simple Heitler-London picture would predict the interaction to be antiferromagnetic as we indeed find to be the case. With this identification of the type of exchange interactions, we may expect that if we dope the band with fewer electrons, then, at some point, the indirect superexchange will switch to ferromagnetic double exchange along the chain based on the Anderson-Hasegawa model [55]. In a later section (Sec. III C 2), we will determine the critical doping level where this crossover to ferromagnetism occurs. The above analysis of the nature of the exchange interactions is similar to that by Horsch and Mack [56].

We may further compare our exchange interactions with previous work in literature. For example, Fan *et al.* [57] reported $J_\parallel$, which is our J_3 to be -51.1 meV or -593 K. However, they considered a $S = 1/2$ spin-Hamiltonian instead of a classical unit-vector spin Hamiltonian so due to this different normalization our values are a factor four smaller. Furthermore they counted each pair only once, whereas our definition of the spin-Hamiltonian counts each pair twice. In fact, their energy difference $E(\mathrm{FM}) - E(\mathrm{AFM}) = 25$ meV per formula unit, i.e., per V pair. This means 100 meV per eight-atom cell, compared to our 139 meV. The difference however is that we attribute this in part to the exchange interactions in adjacent chains, which is present in the ferromagnetic case but cancels in the antiferromagnetic case, whereas they attribute it solely to the interactions between V in the single ladder. Our FM-AFM energy difference per pair of V atoms, or per formula unit is 34.75 meV or 403 K. Our value for the parameter $J_\parallel$ as reported by Fan *et al.* [57] would be -806 K. In fact, in literature, values between -529 and -928 K were reported for this parameter in de Graaf *et al.* [58] based on various computational estimates and experimental values. References to the rest of the literature on exchange interactions in NaV_2O_5 can be found there.

C. Band structure of V_2O_5 doped by carrier injection

In this section, we try different alternative ways of doping V_2O_5 compared with NaV_2O_5. Our goal here is twofold. First, we want to explore how different or similar the resulting band structures are to those of NaV_2O_5. Secondly, we want to view these as simulating doping by gating and determine which approach most closely achieves this and could be used to simulate continuous variation of the electron concentrations ranging from $0 < x < 1$ in the bonding xy band.

1. Background versus Virtual crystal approximation

First we keep the filling of the band the same as in NaV_2O_5. That is two electrons are added per unit cell or one per V_2O_5 unit, or 1 electron per rung in the ladder in the xy-bonding band. The first approach is to compensate the two electrons by a uniform positive background $QB = 2$. The second approach we consider is to compensate the electronic charge by spreading it over the vanadium nuclei. We call this the virtual crystal approximation (VCA). It means we replace the atomic number of V by $Z = 23.5$. In Fig. 9, we show the band structures in the $0.38\Delta\Sigma$ model for the background and for the VCA for the AFM ordered case. These should be compared with the corresponding NaV_2O_5 case in Fig. 4.

We can see in Table IV that the splitting between the occupied d band and the oxygen VBM reduces from the $QB = 2$ to NaV_2O_5 to the VCA case. This can be explained from the differences in electrostatic potential. In the VCA case, we place the compensating positive charge on the vanadium very close to where the electrons in this band are localized. So, the electrons feel a stronger attractive potential, pulling this band down. In the NaV_2O_5 case, the compensating positive charge is residing on the Na^+ ions in the interstitial region between the layers. Compared to the VCA, clearly the attractive potential will be weaker. Finally, if we spread the positive charge out homogeneously in a background, the electrostatic interaction is even weaker, even though some of the charge now resides in the V_2O_5 layer and some in the interstitial, both are smeared out. The same trend is observed in the ferromagnetic band structures. Also similar results are found for our LSDA+U model.

We also examined how these different models affect the magnetic ordering. We focus here only on the ordering of moments along the chain. We find that in the background model, the ordering is still antiferromagnetic but in the VCA case it becomes ferromagnetic or very close to equal energy for ferromagnetic and antiferromagnetic ordering.

TABLE IV. Oxygen p to vanadium d_{xy} band energy difference (eV) in different doping models with $QSGW$ $0.38\Delta\Sigma$.

VCA	NaV_2O_5	$QB = 2$
1.00	2.02	2.53

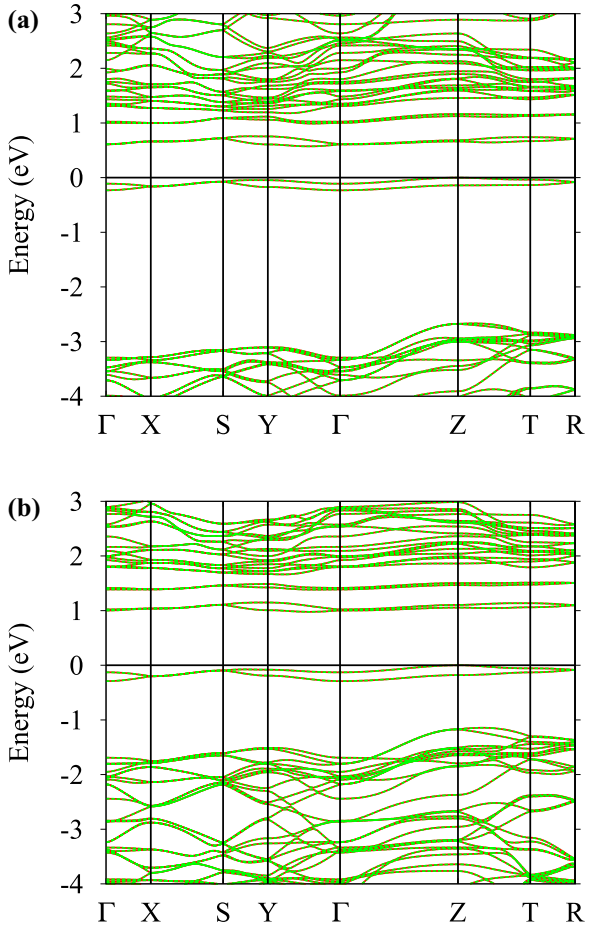

FIG. 9. (Color online) Band structures of AFM doped V_2O_5 with (a) homogeneous background $QB = 2$ in upper figure and (b) VCA by using V with $Z = 23.5$. Both are obtained within $QSGW$ with $0.38\Delta\Sigma$.

Finally, we should note that in the background and VCA models, we used the original V_2O_5 structure which differs slightly from the NaV_2O_5 structure. The **c** lattice constant is somewhat smaller and the pyramids around vanadium are not rotated toward the Na interstitial site. This leads to a slightly smaller band width of the filled split-off band in the ferromagnetic case.

From all this, we conclude that the background model seems more appropriate than the VCA in which compensating charge is placed right on the layer in the V atoms because the latter would yield incorrect predictions about the magnetic order. If we think about a model for injecting charge from a gate, the latter could consist for example of a metallic layer above and below the atomically thin V_2O_5 film. This means the opposite positive charge should stay away from the layer. The background model somewhat achieve this but not quite as accurately as Na itself. In the next section, we therefore consider applying the VCA to Na instead. If we replace $Z = 11$ of Na by $Z = 11 - x$, we simulate in some sense a reduced concentration of Na atoms, we could think about it as replacing some of the Na by inert Ne atoms with $Z = 10$. This could also be viewed as a model for a metallic layer which injects charge into V_2O_5.

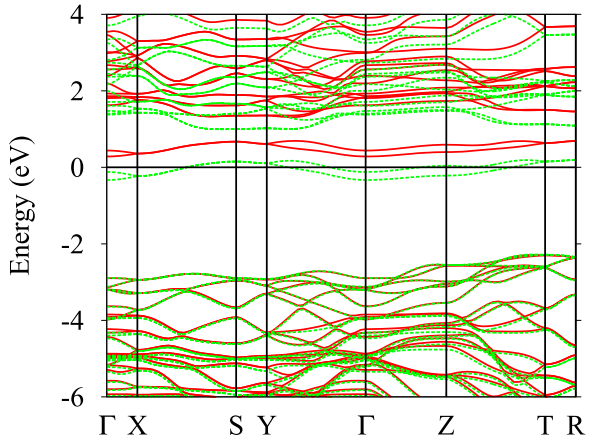

FIG. 10. (Color online) Band structure of background doped V_2O_5 for $QB = 1$, which is ferromagnetic in $QSGW$ with $0.38\Delta\Sigma$.

2. *Continuous doping models*

In this section, we present results for QB doping with $QB = 1$ and 0.5 and also calculations with a VCA for Na atoms with Z continuously varying from 10 to 11.

For $QB = 1$ as shown in Fig. 10, we find as expected a ferromagnetic metallic band structure, with the partially filled band fairly close (about 1 eV) from the CBM. The distance to the VBM depends as before on whether we use LSDA, LSDA+U, $QSGW$, or $0.38\Delta\Sigma QSGW$ + lattice polarization effect. The exchange splitting Δ_x is smaller in LSDA than in GW and is also reduced further if we reduce the background charge to 0.5 (not shown). The exchange splitting Δ_x varies from 1.07 to 0.59 to 0.21 eV for $QB = 2$, 1, 0.5 respectively. Antiferromagnetic structures are less stable in this case. So, this already predicts that for small filling of the band, ferromagnetic coupling could occur but there might be a minimum filling required before the exchange splitting Δ_x is sufficiently large to keep the two bands separate and the half-metallic character preserved. For too small doping, we might simply revert to a nonmagnetic filling of the band.

On the other hand, we are interested also in the case of nearly filled doping, as could occur for example in slightly underdoping with Na, or in the case of Na doping but extracting some electrons out of the layer by gating. In that case, we would start from an AFM ordering along the chains but could locally convert it to FM ordering if we achieve a critical reduction in carrier concentration in the band. This we study by means of NaV_2O_5 with $10 \leqslant Z_{Na} \leqslant 11$ VCA. The magnetic moment of vanadium [shown in Fig. 11(c)] approaches zero for $Z_{Na} \to 10$. This would indicate ferromagnetic ordering even for very small doping of the band. The width of split-off band Δ_x also varies almost linearly with Z_{Na} going from 11 to 10 as shown in Fig. 11(b). However, in reality instead of having a very small spread-out itinerant moment, one might expect localized moments too far from each other to interact. There would thus be some kind of percolation cut-off and one might expect $Na_xV_2O_5$ for small x to be paramagnetic instead of ferromagnetic. This is indeed found to be the case for $Na_{0.33}V_2O_5$ in Chakraverty *et al.* [59]. On the other hand, there is a crossover between the two competing magnetically ordered states (AFM1 and FM) at $Z = 10.88$. This is shown

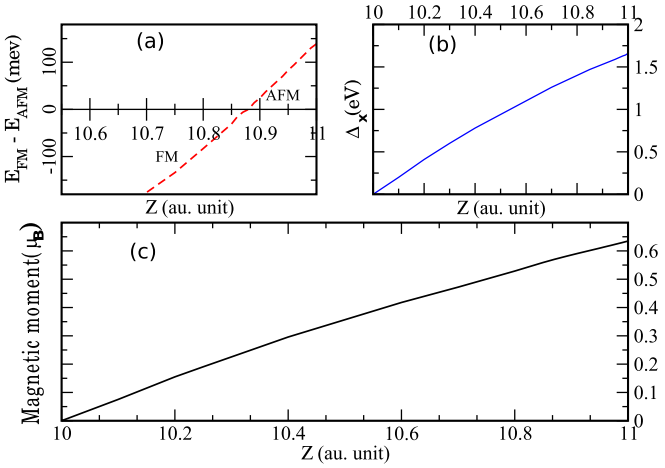

FIG. 11. (Color online) (a) Variation of energy difference E_{FM}-E_{AFM}, (b) split-off band width Δ_x, and (c) magnetic moment per vanadium atom as a function of Z, respectively.

in Fig. 11(a). The band structure becomes metallic for carrier concentration between 0.9 and 1.0 in the split-off d_{xy} bonding band even though the system is antiferromagnetically ordered. This is shown in Fig. 12, which shows a close up of the bands near the Fermi energy. One can see a slight splitting of the up and down spin bands, which also results in a slightly different up and down magnetic moment. This indicates already some gradual transition to the ferromagnetic configuration. Strictly speaking this system is found to be ferrimagnetic in our calculation but the changes in moment are close to the numerical uncertainty of the self-consistent calculation.

IV. CONCLUSIONS

In this paper we studied doping of the V_2O_5 split-off conduction band, first by means of intercalation with Na as in the bronze NaV_2O_5 using first-principles calculations. We found that the half-filling leads to a spin-splitting of this band of about 2 eV within the $QSGW$ method or $QSGW$ method with lattice-polarization correction, as applied previously to pure V_2O_5. This agrees well with the results of LSDA+U

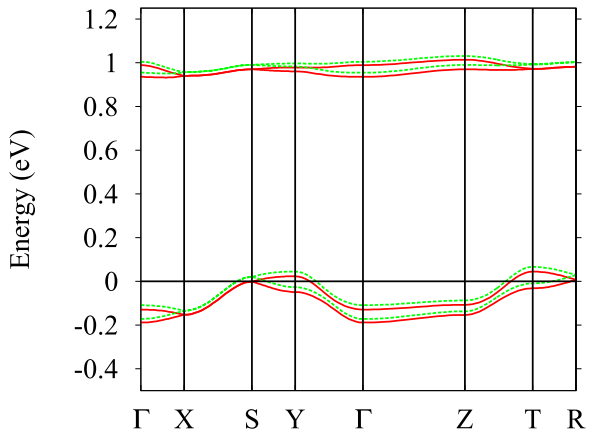

FIG. 12. (Color online) Band structure of metallic $Na_{0.9}V_2O_5$ AFM calculated in LSDA+U.

with $U_{\mathrm{eff}} \approx 2.7$ eV. This further induces spin-splittings of the higher lying conduction bands. This corresponds to a magnetic moment of $1\mu_B$ per V-O^{bridge}-V rung. These moments are found to order antiferromagnetically along the chain and of course, the effective moments of 0.5 μ_B on the V atoms on the same rung are found to prefer strongly to be parallel. However, the staggered neighboring chains or ladders are also found to order antiferromagnetically. The exchange interaction between V atoms along the chain is found to be smaller than the exchange interaction between V in the adjacent chains. The former is an antiferromagnetic superexchange while the latter is a direct V-V interaction. Both contribute to the energy difference from the ferromagnetic state. The FM-AFM energy difference per formula unit is found to be within the range of values previously reported in literature by both experimental determinations and other computations. However, our analysis of the intrachain and interchain exchange interactions differs from previous results, in which either the interchain interaction is neglected or found to be ferromagnetic. Our exchange interactions were extracted from comparing various spin configurations within the LSDA+U model with the U_{eff} value justified by both agreement with the parameter-free $QSGW$ method and optical experiments on the AFM model.

The band structure in the antiferromagnetic ground state is found to have much smaller band widths of the split-off bands, which is explained by the fact that in the AFM case, hopping between nearest neighbors along the chain is prohibited because they have opposite spin. Above the filled band, new states split-off from the continuum. One of these is the antibonding d_{xy} band and the other is the opposite spin counter-part of the bonding d_{xy} band. Both actually result in two bands because of the two chains per unit cell. Optical transitions between the filled d_{xy} band to these empty split-off bands result in two closely spaced peaks in optical conductivity for $\mathbf{E} \parallel \mathbf{a}$ polarization and $\mathbf{E} \parallel \mathbf{b}$. The former correspond to transitions between bonding and antibonding d_{xy} combinations on the same rung, while the latter corresponds to a transition between the spin-split bands which have both bonding character. More precisely, the latter should be viewed as transitions between alternating V atoms along the chain with the same spin. The latter are therefore weaker than the transitions within the same rung. Optical transitions from O-2p valence bands to these same final empty states are found correspondingly at slightly higher energy for $\mathbf{E} \parallel \mathbf{b}$ than for $\mathbf{E} \parallel \mathbf{a}$. These interpretations of the optical transitions agree closely with previous work in literature. We found that the $QSGW$ method slightly overestimates the bonding-antibonding transition but gives a good value for the spin splitting Δ_x.

Various ways for simulating doping by carriers without adding Na explicitly were studied. We found that the position of the occupied split-off band depends strongly on how the electron doping is compensated. This is explained in terms of the different electrostatics. For example, a homogeneous background provides a less attractive electrostatic potential than Na^+ ions in the interstitial space between the layers, or than placing the counter charge on the V atoms. The splitting between bonding and antibonding d_{xy} orbitals or spin-splitting, however, remains the same as before and is independent of this choice of compensating charge. From the

point of view of simulating doping by gating, the compensating charge should be kept away from the doped layer. This is in fact best achieved by Na atoms in the interstitial. One might view the latter as a metallic contact layer. In order to simulate continuously varying electron doping, we then proposed a virtual crystal approximation treatment in which the atomic number Z_{Na} is varied between 10 and 11, 10 representing inert Ne atoms. This model can then simulate both a reduced Na concentration intercalation or a metallic contact gate which pushes a carrier concentration into the V_2O_5 layer that can be tuned continuously between 0 and 2 per unit cell or 0 and 1 per V_2O_5 formula unit, which is equivalent to one ladder. Within this model, we found that for carrier concentrations less than 0.88 e/formula unit, the ordering of the moments switches from AFM to FM. This is in fact expected on the basis of the Anderson-Hasegawa model where the exchange interactions would switch from AFM superexchange to ferro-magnetic double exchange. The same model predicts FM ordering but with continuously decreasing moments all the way down to zero carrier concentration. However, the latter is unrealistic. One should instead expect that there is a minimum critical concentration before localized moments in the chain reach a percolation threshold. In the present model, these moments behave like an itinerant ferromagnet which looses its moments only when zero concentration is reached.

To a large extent our results confirm previous analysis for NaV_2O_5. However, we emphasize the new perspective that in atomically thin layers alternate approaches than variations in the Na concentration could be used to control the charge and thus induce a change from AFM to FM ordering. With the accessibility of the surface to local probes such as an STM tip, this might lead to the control of the local spin alignment on an atomic scale. We caution, however, that further complicating issues should be considered here, such as the spin-Peierls or charge ordering transition occurring at low temperatures, the imperfect ordering in one-dimension accompanied by spin wave excitation fluctuations at finite temperature, etc. Still, our final conclusion is that this system provides possibly an intriguing playground for manipulating spins on the atomic scale at surfaces.

ACKNOWLEDGMENTS

This work was supported by the Air Force Office of Scientific Research under Grant number FA 9550-12-1-0441 (CB) and the US Department of Energy, Office of Science, Basic Energy Sciences, under Grant No. ER-46874-SC0008933 (WL). The strongly correlated NaV_2O_5 aspects of the work and investigation of the $QSGW$ methodology to new systems were supported by DOE while the complex 2D oxide electronics aspects were supported by AFOSR. The calculations were performed at the High Performance Computing Resource in the Core Facility for Advanced Research Computing at Case Western Reserve University.

[1] C. Bhandari, W. R. L. Lambrecht, and M. van Schilfgaarde, Phys. Rev. B **91**, 125116 (2015).
[2] H. Smolinski, C. Gros, W. Weber, U. Peuchert, G. Roth, M. Weiden, and C. Geibel, Phys. Rev. Lett. **80**, 5164 (1998).
[3] W. Lambrecht, B. Djafari-Rouahni, and J. Vennik, J. Phys. C **14** (1981).
[4] G. Bauer, V. Güther, H. Hess, A. Otto, O. Roidl, H. Roller, and S. Sattelberger, Vanadium and Vanadium Compounds in *Ullmann's Encyclopedia of Industrial Chemistry* (Wiley-VCH, Weinheim, 2005).
[5] M. Ponzi, C. Duschatzky, A. Carrascull, and E. Ponzi, Appl. Catal. A **169**, 373 (1998).
[6] A.-M. Cao, J.-S. Hu, H.-P. Liang, and L.-J. Wan, Angew. Chem., Int. Ed. Engl. **44**, 4391 (2005).
[7] C. Wu and Y. Xie, Energy Environ. Sci. **3**, 1191 (2010).
[8] S. F. Cogan, N. M. Nguyen, S. J. Perrotti, and R. D. Rauh, Proc. SPIE **1016**, 57 (1989).
[9] G. Nadkarni and V. Shirodkar, Thin Solid Films **105**, 115 (1983).
[10] Z. R. Xiao, G. Y. Guo, P. H. Lee, H. S. Hsu, and J. C. A. Huang, J. Phys. Soc. Jpn. **77**, 023706 (2008).
[11] M. Isobe and Y. Ueda, J. Phys. Soc. Jpn. **65**, 1178 (1996).
[12] C. Haas, Phys. Rev. **125**, 1965 (1962).
[13] E. O. Kane, Phys. Rev. **131**, 79 (1963).
[14] K. F. Berggren and B. E. Sernelius, Phys. Rev. B **24**, 1971 (1981).
[15] T. S. Moss, Proc. Phys. Soc. London, Sect. B **67**, 775 (1954).
[16] E. Burstein, Phys. Rev. **93**, 632 (1954).
[17] Y. Ueda and M. Isobe, J. Magn. Magn. Mater. **177-181**(Part 1), 741 (1998).
[18] W. Mumme and J. Watts, J. Solid State Chem. **3**, 319 (1971).
[19] Y. Kanke, K. Kato, E. Takayama-Muromachi, and M. Isobe, Acta Crystallogr. Sect. C **46**, 536 (1990).
[20] A. Casalot, D. Lavaud, J. Galy, and P. Hagenmuller, J. Solid State Chem. **2**, 544 (1970).
[21] S. Anderson, Acta. Chem. Scand. **19**, 1361 (1965).
[22] A. Carpy, A. Casalot, M. Pouchard, J. Galy, and P. Hagenmuller, J. Solid State Chem. **5**, 229 (1972).
[23] I. S. Jacobs, J. W. Bray, H. R. Hart, L. V. Interrante, J. S. Kasper, G. D. Watkins, D. E. Prober, and J. C. Bonner, Phys. Rev. B **14**, 3036 (1976).
[24] J. C. Bonner and M. E. Fisher, Phys. Rev. **135**, A640 (1964).
[25] L. N. Bulaevskii, Sov. Phys. JETP **17**, 684 (1963).
[26] F. D. M. Haldane, Phys. Rev. B **25**, 4925 (1982).
[27] F. D. M. Haldane, Phys. Rev. Lett. **50**, 1153 (1983).
[28] M. Hase, I. Terasaki, and K. Uchinokura, Phys. Rev. Lett. **70**, 3651 (1993).
[29] A. Meetsma, J. L. De Boer, A. Damascelli, J. Jegoudez, A. Revcolevschi, and T. T. M. Palstra, Acta Crystallogr. Sect. C **54**, 1558 (1998).
[30] M. Mostovoy and D. Khomskii, Solid State Commun. **113**, 159 (1999).
[31] P. Thalmeier and P. Fulde, Europhys. Lett. **44**, 242 (1998).
[32] J. Lüdecke, A. Jobst, S. van Smaalen, E. Morré, C. Geibel, and H.-G. Krane, Phys. Rev. Lett. **82**, 3633 (1999).
[33] A. I. Smirnov, M. N. Popova, A. B. Sushkov, S. A. Golubchik, D. I. Khomskii, M. V. Mostovoy, A. N. Vasil'ev, M. Isobe, and Y. Ueda, Phys. Rev. B **59**, 14546 (1999).
[34] N. Suaud and M.-B. Lepetit, Phys. Rev. Lett. **88**, 056405 (2002).

[35] A. Bernert, P. Thalmeier, and P. Fulde, Phys. Rev. B **66**, 165108 (2002).
[36] L. Hozoi, A. H. de Vries, A. B. van Oosten, R. Broer, J. Cabrero, and C. de Graaf, Phys. Rev. Lett. **89**, 076407 (2002).
[37] D. O. Scanlon, A. Walsh, B. J. Morgan, and G. W. Watson, J. Phys. Chem. C **112**, 9903 (2008).
[38] C. Bhandari and W. R. L. Lambrecht, Phys. Rev. B **89**, 045109 (2014).
[39] M. Methfessel, M. van Schilfgaarde, and R. A. Casali, in *Electronic Structure and Physical Properties of Solids. The Use of the LMTO Method*, edited by H. Dreyssé, Lecture Notes in Physics Vol. 535 (Springer Verlag, Berlin, 2000), p. 114.
[40] T. Kotani and M. van Schilfgaarde, Phys. Rev. B **81**, 125117 (2010).
[41] W. Kohn and L. J. Sham, Phys. Rev. **140**, A1133 (1965).
[42] U. von Barth and L. Hedin, J. Phys. C **5**, 1629 (1972).
[43] http://www.lmsuite.org
[44] https://github.com/tkotani/ecalj
[45] M. van Schilfgaarde, T. Kotani, and S. Faleev, Phys. Rev. Lett. **96**, 226402 (2006).
[46] M. van Schilfgaarde, T. Kotani, and S. V. Faleev, Phys. Rev. B **74**, 245125 (2006).
[47] T. Kotani, M. van Schilfgaarde, and S. V. Faleev, Phys. Rev. B **76**, 165106 (2007).
[48] R. Enjalbert and J. Galy, Acta Crystallogr. Sect. C **42**, 1467 (1986).
[49] J. F. Janak, Phys. Rev. B **16**, 255 (1977).
[50] M. N. Popova, A. B. Sushkov, S. A. Golubchik, B. N. Mavrin, V. N. Denisov, B. Z. Malkin, A. I. Iskhakova, M. Isobe, and Y. Ueda, Zh. Eksp. Teor. Fiz. **115**, 2170 (1999) [J. Exp. Theor. Phys. **88**, 1186 (1999)].
[51] X. Ming, H.-G. Fan, Z.-F. Huang, F. Hu, C.-Z. Wang, and G. Chen, J. Phys.: Condens. Matter **20**, 155203 (2008).
[52] M. J. Konstantinović, Z. V. Popović, V. V. Moshchalkov, C. Presura, R. Gajić, M. Isobe, and Y. Ueda, Phys. Rev. B **65**, 245103 (2002).
[53] S. Atzkern, M. Knupfer, M. S. Golden, J. Fink, A. N. Yaresko, V. N. Antonov, A. Hübsch, C. Waidacher, K. W. Becker, W. von der Linden, G. Obermeier, and S. Horn, Phys. Rev. B **63**, 165113 (2001).
[54] C. Presura, D. van der Marel, A. Damascelli, and R. K. Kremer, Phys. Rev. B **61**, 15762 (2000).
[55] P. W. Anderson and H. Hasegawa, Phys. Rev. **100**, 675 (1955).
[56] P. Horsch and F. Mack, Eur. Phys. J. B **5**, 367 (1998).
[57] H.-g. Fan, X. Ming, F. Hu, C.-z. Wang, Z.-f. Huang, and G. Chen, Chem. Res. Chin. Univ. **25**, 243 (2009).
[58] C. de Graaf, L. Hozoi, and R. Broer, J. Chem. Phys. **120**, 961 (2004).
[59] B. K. Chakraverty, M. J. Sienko, and J. Bonnerot, Phys. Rev. B **17**, 3781 (1978).